SIMULATION OF OLIVE PITS PYROLYSIS IN A ROTARY KILN PLANT

by

Enzo BENANTI [a], ***Cesare FREDA*** [b*], ***Vincenzo LOREFICE*** [c]
Giacobbe BRACCIO [b], ***and Vinod Kumar SHARMA*** [b]

[a] Facoltà di Ingegneria,Università degli Studi di Catania, Catania, Italy
[b] ENEA, UTTRI-BIOM, Rotondella (MT), Italy
[c] SICARB Srl, Priolo Gargallo (SR), Italy

Original scientific paper
UDC: 662.756:66.092-977
DOI: 10.2298/TSCI090901073B

This work deals with the simulation of an olive pits fed rotary kiln pyrolysis plant installed in Southern Italy. The pyrolysis process was simulated by commercial software CHEMCAD. The main component of the plant, the pyrolyzer, was modelled by a plug flow reactor in accordance to the kinetic laws. Products distribution and the temperature profile was calculated along reactor's axis. Simulation results have been found to fit well the experimental data of pyrolysis. Moreover, sensitivity analyses were executed to investigate the effect of biomass moisture on the pyrolysis process.

Key words: *pyrolysis, rotary kiln, agricultural residue, biomass, char, biooil, kinetic, plug flow reactor*

Introduction

Pyrolysis is a complex chemical process that happens when a matrix, usually organic, is heated in inert atmosphere. The thermal energy, supplied to the organic matrix, breaks part of chemical bonds to give solid, liquid, and gas. The solid, called "char", is mainly composed of carbon, hydrogen, and oxygen along with little percentage of metallic elements. The liquid component is a mixture of water and oxygenated organic compounds (here onward biooil) such as carboxylic acids, alcohols, ketones, aldehydes, hydrocarbons, *etc*. Finally, pyrolysis gas is composed of hydrogen, carbon monoxide, carbon dioxide, methane, and other light hydrocarbons. The relative amounts of pyrolysis products depends on the operating temperature, heating rates and residence times in the reactor of the chemical species involved in the process. Operating temperature of 300-400 °C and long residence time of the biomass (up to hours), increases char production up to 35% (slow pyrolysis). Contrary, at higher operating temperature, *i. e.* 800-900 °C and adopting residence times long enough to crack the organic vapours (some tens of seconds), the amount of gas increases up to 85% (tab. 1). Short residence times (up to few seconds) followed by rapid quenching of pyrolysis vapours, are used to obtain main product, the biooil (fast-pyrolysis) [1].

* Corresponding author; e-mail: cesare.freda@enea.it

Table 1. Relative distribution of different pyrolysis products *vs.* temperature

	Temperature [°C]	Liquid [wt.%]	Solid [wt.%]	Gas [wt.%]
Slow pyrolysis	300-400	30	35	35
Fast pyrolysis	450-600	75	12	13
High temperature pyrolysis	800-900	5	10	85

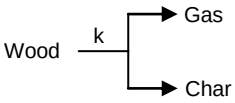

Figure 1. One step model of Kung

Kinetic models of biomass pyrolysis were developed in early Seventies. In 1972 Kung [2] proposed a model based on one step (fig. 1) considering pyrolysis as a first order reaction with decomposition of biomass into fixed char yield compared to the gas yield. Here, the char reactions with the pyrolysis gas, such as carbon dioxide, water, hydrogen, *etc*. are neglected. In Kung's work, theoretical data was not compared to the experimental ones. Thereafter several authors have adopted the one step model, Miyanami *et al.* [3], Fan *et al.* used it in their volume reaction model [4]. Recently, Peters *et al.* realized a numerical method to describe heating-up, drying, and pyrolysis of large wood particles on one step model with a first order reaction [5].

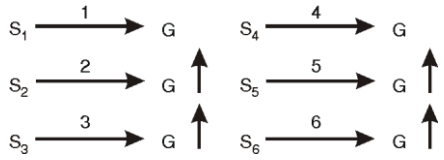

Figure 2. One step multi-reactions model of Alves

Alves *et al.* [6], in their study identified six macro constituents of pine sawdust: hemicellulose, cellulose, lignin, and three variously degraded lignin. For very small particles, having negligible internal temperature gradients, these authors set up a model with six parallel first order reactions (fig. 2), each one involving the volatile part of each macro constituent of the starting material. This model, just like other models with one step and one pyrolysis reaction [2-5], gives a fixed char yield compared to gas yield and does not consider secondary reactions of primary pyrolysis products.

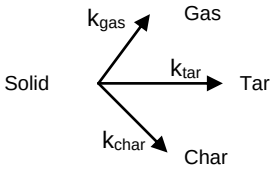

Figure 3. One step multi competing reactions model of Thurner

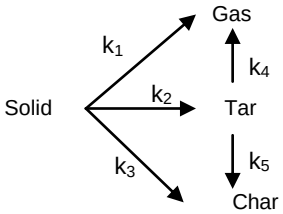

Figure 4. Two step multi competing reactions model of Di Blasi

Thurner *et al*., in 1981 [7], used a more realistic approach (as suggested by Shafizadeh in 1977 [8]): one step model with three parallel and competing first order reactions (fig. 3). The kinetics of wood pyrolysis into gas, tar, and char was investigated in the range of 300 to 400 °C at atmospheric pressure. The secondary reactions of pyrolysis were included in the kinetic laws of primary reactions. In this way the char yield varies compared to tar and gas yield. Recently, this approach has been used by Shen *et al.* [9] to model pyrolysis of wet wood under heat flux.

Di Blasi modelled the pyrolysis behaviour of a shrinking biomass particles [10]. Author proposed a model with two steps: the first describes the primary degradation of the solid biomass whereas the second describes the degradation of tar formed by primary pyrolysis step (fig. 4).

Experimental work of Broido *et al.* showed that cellulose pyrolysis occurs according to multistep decomposition thus yielding several degradation products such as 1,6-anhydroglucose, 1,5-anhydro-4-deoxy-D-glycero-hex-1-en-3-ulose, 5-hydroxymethyl-2 furfural, and levoglucosenone [11]. Later, taking into account the work reported by Broido *et al.* [11], Shafizadeh *et al.* [12], proposed a simplified reaction model about pyrolysis of cellulose often called as "Broido-Shafizadeh model". The model, in question, can be described by two steps (fig. 5). It was assumed that an "initiation reaction" leads to formation of an "active cellulose" which subsequently decomposes into two competitive first-order reactions, one yielding volatiles and the other yielding char and gas.

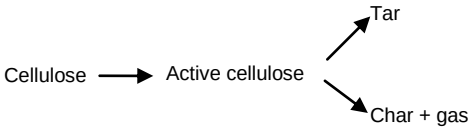

Figure 5. Two step model of Shafizadeh

This scheme was widely adopted by several authors. For example, Liden *et al.* [13] simulated kinetically the production of liquid from flash pyrolysis of biomass. Moreover, he enriched the Broido-Shafizadeh model, assuming that the volatile react by secondary homogeneous reactions to form gas as a main product.

Koufopanos in 1991 modelled biomass pyrolysis according to scheme (fig. 6). This model indicates that biomass decomposes to primary pyrolysis products according to competitor reactions one yielding primary gas and volatile and the other yielding primary char. Gas and volatile react with char in a secondary pyrolysis step to give volatile, gas, and char of different composition. Thus, the primary pyrolysis products participate in secondary interactions causing a modified final product distribution. This model was often adopted by other authors [15, 16].

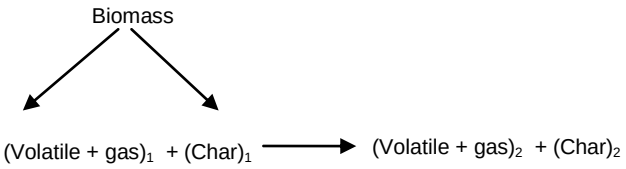

Figure 6. Two step model of Koufopanos

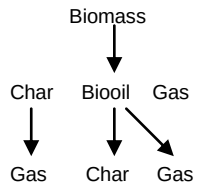

Figure 7. Two step model adopted in this work

This introduction on chemical schemes used to describe pyrolysis process shows that multistep schemes, having secondary pyrolysis step, are more realistic compared to models having only primary pyrolysis step. In this study an original approach was considered. Chemical scheme adopted (fig. 7), consists of two steps. The first describes the primary pyrolysis of solid biomass, that gives char, biooil, and gas, according to a first order reaction. In the second step the products of the primary pyrolysis, char, biooil, and gas are involved in competing reactions of: char gasification, biooil reforming, and biooil charring.

Facility and experimental data

In Siracusa district of Sicily, in Southern Italy, a rotary kiln pyrolizer of Sicarb Srl is in operation in the slow pyrolizing. The main purpose is to convert olive pits into char fated to the production of activated char. The innovation of this plant is that no waste has to be managed in the productive cycle.

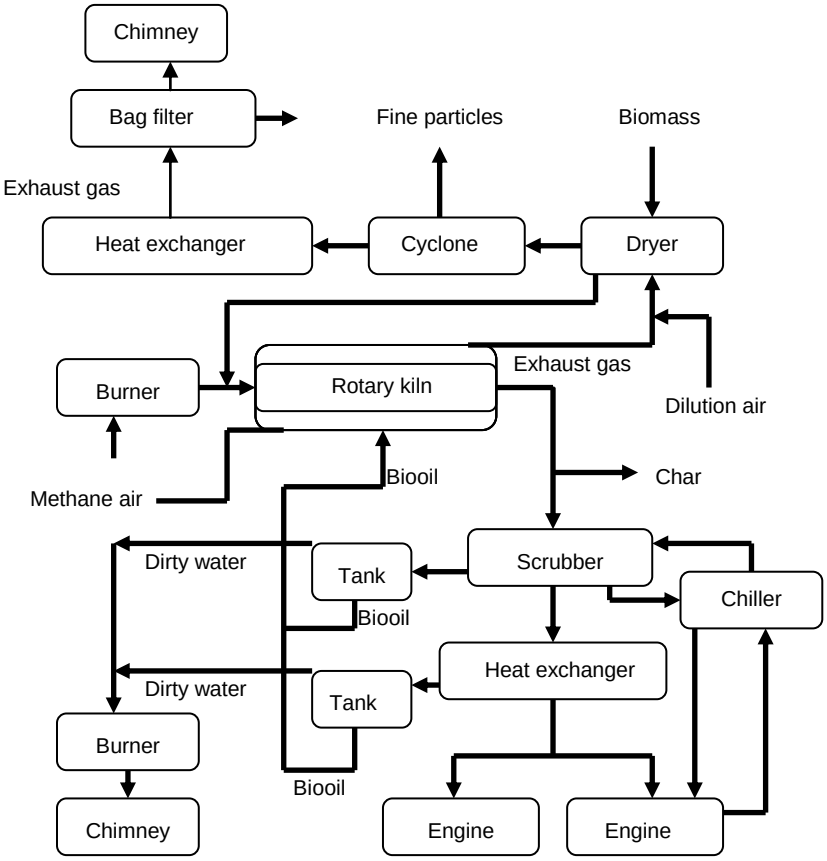

Figure 8. Flow sheet of the pyrolysis plant

Figure 8 shows a flow sheet of the pyrolysis plant. About 2000 kg/h of wet olive pits at 15% are dried in a rotary dryer up to moisture content of 5%. Dried biomass is fed into the rotary kiln pyrolyzer (length 20 m, internal diameter 1.6 m), where at temperature of about 500 °C, it is converted into char and co-products such as organic vapours, water, and incondensable gas (carbon monoxide, carbon dioxide, hydrogen, and light hydrocarbons). The inert atmosphere in the rotary kiln is maintained by an exhaust flux of combustion (carbon dioxide, water, and nitrogen) of about 10 kg/h of methane, that occurs in a burner by air. The solid char is convoyed to a reactor at 900 °C where it is activated by oxygen and/or water steam. Thus the specific area of the char is increased with beneficial effect on its adsorbing capacity.

The co-products of slow-pyrolysis are washed in a scrubber and cooled down to 70 °C in a heat exchanger. At this temperature biooil and water condense, and they are separated by decantation in two tanks, each one communicating with the scrubber and heat exchanger. The biooil and certain amount of methane is burnt in the shell of the rotary kiln to sustain the pyrolysis. The produced exhaust gas flows concurrently with the pyrolysis products. In addition, the exhaust gas suitably diluted using air was used to dry the biomass. The water,

polluted by organic hydrophilic compounds, flows through a methane burner where the organic molecules are burnt.

The syngas, after successive washing and filtration, is burnt in two endothermic engines GE Jenbacher of 1176 kW_e. Thermal energy recovered from the engines sustains the chiller that cool the liquid (biooil and water) for scrubber.

To determine the accurate distribution of pyrolysis products (tab. 2 and fig. 13), experimental tests were conducted using nearly 2000 kg/h of olive pits at 15% initial moisture content. Methane was burnt in the shell of rotary kiln to supply energy required for the pyrolysis. It is worth to mention that moisture content of the olive pits was reduced to nearly 5%. At the end of this tests by gravimetric method, amount of char, bio-oil and water were measured. The amount of syngas was calculated by closure of mass balance. The dry syngas composition was measured downstream of the heat exchanger by an on-line gas-chromatograph system Agilent Technologies working with double column, (back flush system) molecular sieve 5A and PoraplotQ, argon as gas carrier, and thermal conductivity detector. Identification of each component is based on retention time and multilevel external calibration. The low heating values of char and biooil were measured by calorimetric bomb according to UNI CEN/TS 14918 method, whilst the low heating value of syngas was calculated.

Table 2. Distribution of pyrolysis products: experimental data

	Char	Biooil	Water	C_2H_4	CO_2	H_2	CO	CH_4
Weight [%]	38	10	6	1	15	1	23	6
LHV [MJ/kg]	29	30	–	15				

Model description

The first step to approach simulation by software CHEMCAD was the definition of chemical species involved in the process. The biomass was assumed to be a pseudo-compound formed by carbon, hydrogen, and oxygen ($C_\alpha H_\beta O_\chi$) in amount, agreement with the data reported in the literature [17]. The brute molecular formula assumed for the biomass is $C_{100}H_{120}O_{40.}$ Its specific heat was assumed to be function of temperature according the Koufopanos *et al*. formula [14]:

$$C_p\,[\mathrm{Jkg^{-1}K^{-1}}] = 1112 + 4.85\ T[\mathrm{K}] - 273 \tag{1}$$

Knowing, experimental heating value of the biomass (21 MJ/kg_{daf}) and the standard enthalpy formation of products of combustion reaction of the biomass (reaction 2), value of standard enthalpy formation was calculated as (eq. 3):

$$C_{100}H_{120}O_{40} + 110\ O_2 = 100\ CO_2 + 60\ H_2O + \Delta H_c \tag{2}$$

$$\Delta H_f^\circ(C_{100}H_{120}O_{40}) = 100\Delta H_f^\circ(CO_2) + 60\ \Delta H_f^\circ\ H_2O\ + \Delta H_c \tag{3}$$

The biooil, in SICARB plant, as already mentioned, is burnt to sustain energetically the pyrolysis. The same was simulated by a liquid substance (n-propyl alcohol C_3H_8O) having same calorific value as that of biooil (about 29 MJ/kg). The char was simulated by elemental carbon. This assumption is justified by the high amount of carbon of the pyrolysis char, as

Table 3. Chemical species in the simulation

j	Chemical species
1	$C_{100}H_{120}O_{40}$
2	H_2
3	CO
4	CO_2
5	CH_4
6	H_2O
7	C_3H_8O
8	C

reported in previous works [18]. Finally, the syngas, the ethylene was assumed to be methane. Table 3 lists the chemical species considered in the present simulation.

Process layout, simulated by CHEMCAD is reported in fig. 9. The input chemical species are biomass, methane, and air whereas the output are char, water, syngas (CO, H_2, CO_2, CH_4) and exhaust gas of combustion (CO_2, H_2O, N_2) mixed with dilution air. The simulated operation units of the plant are: biomass dryer, biomass pyrolyzer, methane, and biooil burners.

The dryer module simulates the material and energy balances associated with biomass drying process. Temperature and moisture degree of the dried outgoing biomass are fixed and the thermal power subtracted, to the exhaust gas of biooil combustion mixed with dilution air, is calculated.

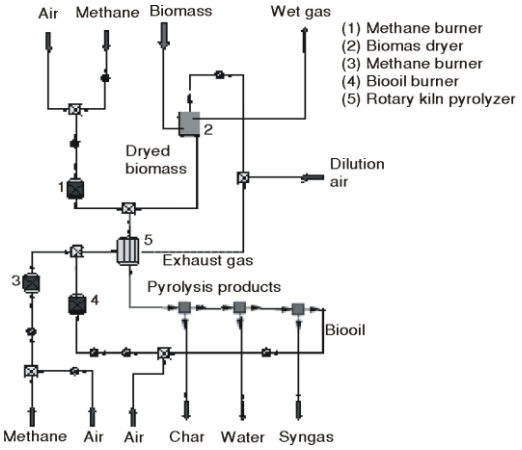

Figure 9. Simulation layout by CHEMCAD

The methane burnt by air, fated to inert atmosphere generation, is simulated by a unit, where mass and energy balances associated with methane stoichiometric combustion occur (reaction 4).

$$CH_4 + 2O_2 \rightarrow CO_2 + 2H_2O \tag{4}$$

This unit simulates a power loss equal to 20% of inlet methane power. The inert flux of methane combustion and dried biomass are adiabatically mixed before to get into the pyrolyzer.

It was assumed that the rotary kiln pyrolyzer works under a thermally thin regime, so temperature is nearly constant across the biomass and char particles. Moreover, mass transfer and diffusion were considered faster than chemical reactions; thence the kinetics of chemical reactions control the rate of phenomenon. Considered chemical reactions are:

$$C_{100}H_{120}O_{40} \leftrightarrow 66.976C + 6.203C_3H_8O + 17.136H_2O + 9.734H_2 + 3.852CO + 6.404CO_2 + 4.159CH_4 \tag{5}$$

$$C + CO_2 \leftrightarrow 2CO \tag{6}$$

$$C + H_2O \leftrightarrow H_2 + CO \tag{7}$$

$$C + 2H_2 \leftrightarrow CH_4 \tag{8}$$

$$H_2O + CH_4 \leftrightarrow CO + 3H_2 \tag{9}$$

$$C_3H_8O \leftrightarrow 3C + H_2O + 3H_2 \tag{10}$$

$$6C_3H_8O + H_2O + 3H_2 \leftrightarrow CO + 3CO_2 + 14CH_4 \tag{11}$$

The kinetic equations of chemical reactions are reported in tab. 4. The seven stoichiometric coefficients of the reaction (5), that is "the primary pyrolysis", were determined solving a mathematical system of seven equations. Three equations are derived from the mass balances of carbon hydrogen and oxygen whereas others were written in order to satisfy the experimental data obtained by Di Blasi *et al.* [19], who approached the primary pyrolysis stage in their study.

Table 4. Kinetic equations of the chemical reactions

Chemical reactions	Kinetic laws	Authors
(5)	$r_5 = k_5 \cdot C_b \cdot \mathrm{PM}_b$	Bonnefoy *et al*. [20]
(6)	$r_6 = k_6 \cdot \left(P_{CO_2} - \frac{P_{CO}^2}{K_6} \right)$	Wang *et al*. [21]
(7)	$r_7 = k_7 \cdot \left(P_{H_2O} - \frac{P_{CO} \cdot P_{H_2}}{K_7} \right)$	Wang *et al*. [21]
(8)	$r_8 = k_8 \cdot \left(P_{H_2}^2 - \frac{P_{CH_4}}{K_8} \right)$	Wang *et al.* [21]
(9)	$r_9 = k_9 \left(P_{CH_4} \cdot P_{H_2O} - \frac{P_{CO} \cdot P_{H_2}^3}{K_9} \right)$	Wang, *et al*. [21]
(10)	$r_{10} = k_{10} \cdot C_{C_3H_8O} \cdot \mathrm{PM}_{C_3H_8O}$	Di Blasi [22]
(11)	$r_{11} = k_{11} \cdot C_{C_3H_8O} \cdot \mathrm{PM}_{C_3H_8O}$	Liden *et al*. [13]

The reactions (6)-(11) concern the second step of pyrolysis. More precisely, the reactions (6)-(8) describe the gasification of primary char by carbon dioxide, water, and hydrogen, respectively. Reaction (9) takes into account the methane reforming by water. Lastly, reactions (10) and (11), synthesise the charring phenomena of biooil and its reforming to carbon monoxide, carbon dioxide, and methane. The kinetic equations of reactions (5)-(11) as shown in the Arrhenius equation, are function of temperature, *i. e.*

$$k = A \cdot \exp\left(-\frac{E_a}{RT} \right) \tag{12}$$

In the kinetic equations of reactions (6)-(9), the effect of the thermodynamic equilibrium constant (K_i), is considered too. Furthermore, in eqs. (10) and (11), the kinetic constant was corrected multiplying the frequency factor for 0.0001 to fit better the experimental data. Most probably, this correction might be due to heat or mass transfer limitation.

The rotary kiln pyrolyzer was modelled by a plug flow reactor (PFR). The basic assumptions of PFR model are: no axial mixing or axial heat transfer occurs (fluids are perfectly mixed in the radial direction but not in the axial direction). Transit times for all fluid elements through the reactor, from inlet to outlet, are of equal duration. The fluid, going through PFR, might be modelled as flowing through the reactor, as a series of infinitely thin coherent "plugs", each with a uniform composition, travelling in the axial direction of the reactor, with each plug having a different composition from the ones before and after. Each plug with differential volume (dV) is considered as a separate entity, effectively an infinitesimally small batch reactor, limiting to zero volume [23].

In an ideal PFR, concentration is a function of both distance along the flow path, x, and time, t: $C = C(x,t)$.

For a mass balance of a chemical species, taking mass balance on infinitely thin coherent plug with uniform concentration (fig. 10), where dV is the differential volume, A – the cross-sectional area, dx – the differential distance, and Q – the fluid flowrate,

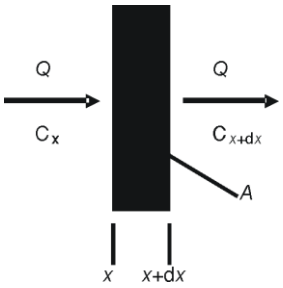

Figure 10. Differential axial element of plug flow reactor

with

$$\text{Accumulation} = \text{In} - \text{Out} + \text{Generation} \tag{13}$$

$$\text{In} = QC_x \tag{14}$$

$$\text{Out} = QC_{x+dx} \tag{15}$$

$$\text{Generation} = dVr = Adxr \tag{16}$$

$$\text{Accumulation} = dV\left(\frac{\delta C_x}{\delta t}\right) = Adx\left(\frac{\delta C_x}{\delta t}\right) \tag{17}$$

Replacing (14)-(17) in (13) it has that:

$$dV\left(\frac{\delta C_x}{\delta t}\right) = QC_x - QC_{x+dx} + dVr \tag{18}$$

As

$$C_{x+dx} = C_x + dC_x \tag{19}$$

Replacing (18) in (17), we have:

$$dV\left(\frac{\delta C_x}{\delta t}\right) = Q(C_x - C_x - dC_x) + dVr \tag{20}$$

$$\left(\frac{\delta C_x}{\delta t}\right) = -Q\left(\frac{\delta C_x}{\delta V}\right) + r \tag{21}$$

$$\left(\frac{\delta C_x}{\delta t}\right) = -\frac{\delta C_x}{\delta\left(\frac{V}{Q}\right)} + r \tag{22}$$

As

$$\delta\left(\frac{V}{Q}\right) = \delta\tau \tag{23}$$

where τ is the hydraulic residence time, at steady-state:

$$\left(\frac{\delta C_x}{\delta t}\right) = 0 \tag{24}$$

Replacing (23) and (24) in (22), it has:

$$\left(\frac{\delta C_x}{\delta t}\right) = r \tag{25}$$

and replacing the partial differential with ordinary one it has the mass balance of a chemical species:

$$\left(\frac{dC_x}{d\tau}\right) = r \tag{26}$$

Considering the seven chemical reactions that describe the phenomenon (5)-(11), and the eight chemical species, it will easy to solve the following system of eight differential equations:

$$\frac{\mathrm{d}C_1}{\mathrm{d}\tau} = -r_5 \tag{27}$$

$$\frac{\mathrm{d}C_2}{\mathrm{d}\tau} = 9.734r_5 + r_7 - 2r_8 + 3r_9 + 3r_{10} - 3r_{11} \tag{28}$$

$$\frac{\mathrm{d}C_3}{\mathrm{d}\tau} = 3.852r_5 + 2r_6 + r_7 + r_9 + r_{11} \tag{29}$$

$$\frac{\mathrm{d}C_4}{\mathrm{d}\tau} = 6.404r_5 - r_6 + 3r_{11} \tag{30}$$

$$\frac{\mathrm{d}C_5}{\mathrm{d}\tau} = 4.159r_5 + r_8 - r_9 + 14r_{11} \tag{31}$$

$$\frac{\mathrm{d}C_6}{\mathrm{d}\tau} = 17.136r_5 - r_7 - r_9 + r_{10} - r_{11} \tag{32}$$

$$\frac{\mathrm{d}C_7}{\mathrm{d}\tau} = 6.203r_5 - r_{10} - 6r_{11} \tag{33}$$

$$\frac{\mathrm{d}C_8}{\mathrm{d}\tau} = 66.976r_5 - r_6 - r_7 - r_8 + 3r_{10} \tag{34}$$

It is obvious from the output of the pyrolysis unit (fig. 9) that the pyrolysis products (char, biooil, water, and syngas) are roughly separated by three serial component separators units. These units work independently from the chemical-physical operability of the separation. the simulations of char separation, co-products scrubbing and quenching, and bio-oil decantation, *etc*., are not the goal of this work, these units can be successfully used.

Biooil combustion by air is simulated by a unit, that simulates a mass and energy balance associated with biooil stoichiometric combustion (reaction 35).

$$C_3H_8O + 4.5O_2 \leftrightarrow 4H_2O + 3CO_2 \tag{35}$$

This unit works with a power loss equal to 20% of inlet biooil power. Pilot flame created by combustion of methane by air, is simulated in the same way.

The exhaust gases from bio-oil and methane combustion are mixed adiabatically and (co-currently to the biomass flow) cross the shell of pyrolysis unit providing the thermal energy for the process. In order to achieve simulation outlet temperature similar to both the experimental outlet temperature of pyrolysis products and exhaust combustion gas temperature, the overall heat transfer coefficient was set equal to 27 W/m^{2}K.

Results and discussion

Temperature and residence time are two fundamental parameters that rule the pyrolysis process. To verify the validity of the proposed model, sensitivity analysis showing the influence of these variables, was performed. Distribution of pyrolysis products as function of the process temperature (50-750 °C) at fixed biomass flowrate of 1700 kg/h and fixed

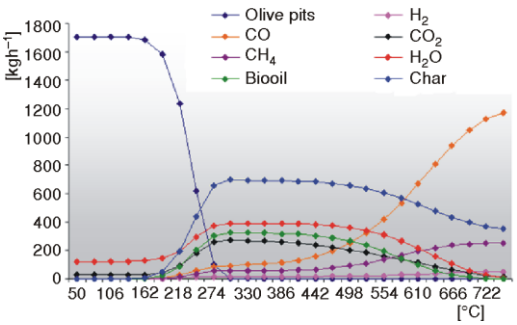

Figure 11. Distribution of pyrolysis products with 1700 kg/h of olive pits *vs.* temperature at 30 minutes of residence time

residence time of the biomass in the reactor equal to 30 minutes (as in the SICARB plant) are shown in fig. 11.

As expected, increase in temperature at fixed residence time of biomass in the reactor, helps in the advancement of chemical reactions. It has been observed that up to 150 °C, the biomass does not undergo any degradation. Above this temperature, the primary pyrolysis starts (reaction 5) and continue till 300 °C. However, with further increasing in temperature, the second step of the pyrolysis starts. This causes an increase of the incondensable gas. Higher residence time shifts the pyrolytic steps towards lower temperature whereas lower residence time shifts them to the higher temperature.

Isothermal pyrolysis runs at 350 and 500 °C, at biomass flowrate of 1700 kg/h, were also performed. The main purpose of this exercise was to demonstrate the effect of residence time of the biomass on the process as well as monitoring the distribution of pyrolysis products.

The results obtained from the isothermal pyrolysis, simulated at 350 °C and biomass flowrate equal to 1700 kg/h (fig. 12) clearly shows that a residence time of thirty minutes, quite enough to finish the primary pyrolysis of olive pits is certainly not sufficient to start the chemical reactions of secondary pyrolysis step. Residence time, shorter than twenty minutes, may have unconverted biomass as pyrolysis product, whose amount could be as higher as shorter is the residence time.

Besides, it is interesting to observe that biomass reduces progressively with the time, exponentially (trend linked to the kinetic model adopted). In other words, reaction rate of primary pyrolysis decreases with reduction of biomass concentration (eq. 5).

Figure 13, evinces how in the isothermal pyrolysis simulated at 500 °C, the amounts of char and biooil decreases with residence time of three minutes. This clearly indicates the beginning of the chemical reactions of secondary pyrolysis – reactions (6)-(11).

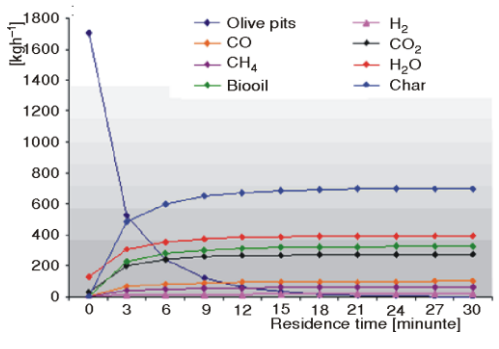

Figure 12. Pyrolysis products of 1700 kg/h of olive pits *vs.* residence time at 350 °C

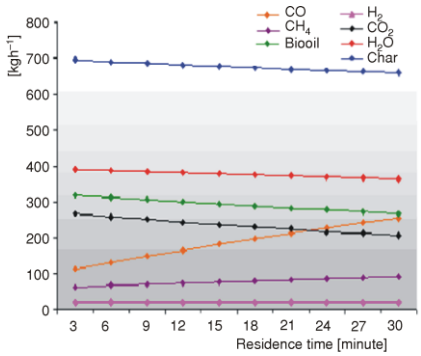

Figure 13. Pyrolysis products of 1700 kg/h of olive pits *vs.* residence time at 500 °C

After having investigated sensitivity of the model to both temperature and the residence time, simulation of SICARB plant operation providing thermal energy to the process by the biooil combustion, has also been performed.

It is evident, from fig. 14, that the results obtained from the model are in good agreement with the experimental data of the SICARB plant. Furthermore, final experimental temperature of output products (520 °C) is very near to the one simulated by the model. Thorough investigations of the results obtained reveals that the simulation provides a maximum relative error equal to +5.1 for water, and –3.5 for carbon dioxide. These differences in the case of carbon dioxide, that could certainly be considered to be negligible, can be attributed to the fact that in the simulation infiltration of air that occurs in the SICARB plant (responsible for the increase of carbon dioxide content by mean of combustion reactions) was not considered. As a proof of this, fig. 14, shows that the combustible carbon monoxide and methane are lightly over predicted by simulation compared to the reality.

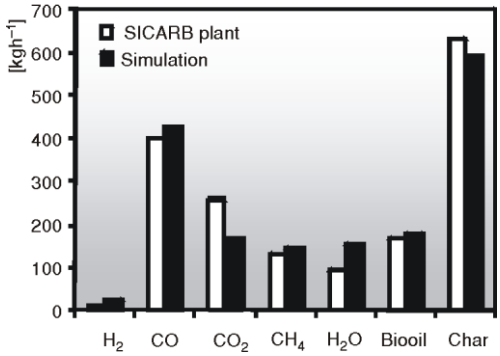

Figure 14. Pyrolysis products of SICARB plant and of the simulation

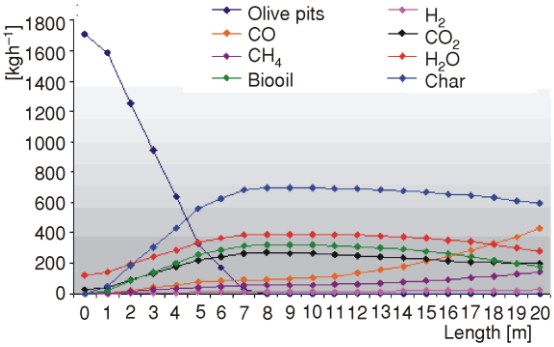

Figure 15. Simulated pyrolysis products *vs.* reactor axis at running condition

The over prediction of water and little amount of hydrogen could be linked to the definition of char adopted in the model. More precisely, char simulated as pure carbon (an assumption adopted by several authors [21, 24, 25]) drives to underestimate the hydrogen and oxygen content in the char. It is evident from the experiments that the situation will certainly be reversed in compounds having high percentage content of hydrogen and oxygen such as water and molecular hydrogen.

In order to investigate what occurs along the axis of the rotary kiln pyrolyzer (approx 20 meter in length) of plant in operation under stationary conditions, sensitivity analysis was performed, as well. Figure 15, shows both the pyrolysis steps, *i. e.* primary pyrolysis of the biomass (up to about 8 meters) and the secondary pyrolysis (that involves char gasification, biooil reforming and charring) takes place after about 8 meters. It is already patent that the maximum char yield comes off when the primary pyrolysis finishes and the secondary one is not started yet. It is therefore to be noted that from the 8 meters onward, amount of char decreases by about 15% but its quality is improved. This could be attributed to gasification reactions – reactions (6)-(8) that increase its superficial area.

The temperature profile is reported in fig. 16. As expected, the temperature rises along the reactor axis because of the thermal energy released by the combustion of biooil. A critical remark underlines an inflection point at about 350 °C located at length of about 8 meters, that matches with the end of the primary pyrolysis. This point and the double

concavity of the curve is justified considering the heat of reactions related to the two pyrolysis steps. The reaction 5, of biomass primary pyrolysis, is strongly endothermic compared to the reactions of the second step.

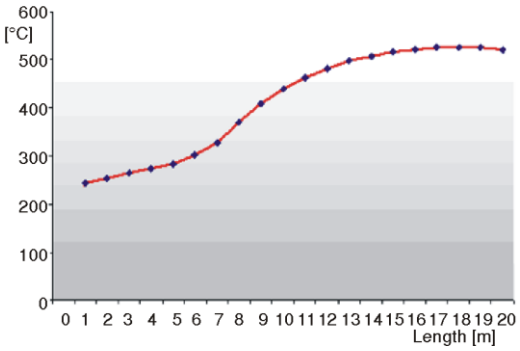

Figure 16. Simulated temperature profile *vs.* the pyrolyzer axis at running condition

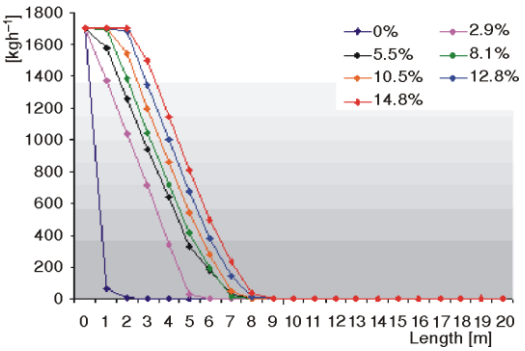

Figure 17. Biomass flowrate *vs.* the pyrolyzer axis at different moisture (weight percentage) of fed biomass to the pyrolyzer

Another analysis was conducted to verify the effect of moisture of biomass on the process, while varying the drying capacity of the dryer and thus feeding the biomass to the pyrolyzer at different moisture content. In this analysis (fig. 17) the moisture content of olive pits that is fed to the pyrolyzer varies from zero (dry biomass) to 14.8% (value quite near to the equilibrium value with the environment). It has been observed that while feeding the pyrolyzer with dry biomass, the primary pyrolysis finishes at about three metres whereas with biomass feeding at moisture content equal to 14.8%, the primary pyrolysis finishes at about 10 metres (fig. 17).

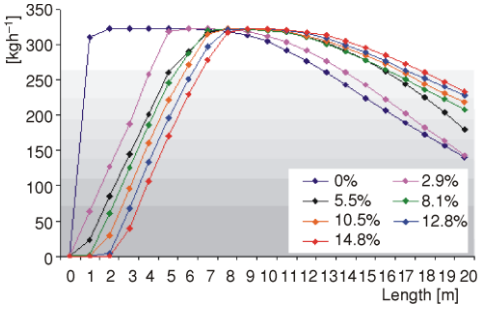

Figure 18. Biooil flowrate *vs.* the pyrolyzer axis at different moisture (weight percentage) of fed biomass to the pyrolyzer

The cited significant difference can be explained by the fact that the more wet biomass compared to the dry one, mainly because of the higher specific heat of the water compared to the biomass, causes a temperature decrease along the pyrolyzer that slows down the kinetics of both primary and secondary pyrolysis. As matter of the fact, as shown in fig. 18 (where the biooil flowrate along the pyrolyzer is reported) considering an inlet biomass equal to 1700 kg/h, at different moisture content, it can be observed that increase of biomass moisture increases the output biooil yield. As the biooil is a reactant of the secondary pyrolysis (fig. 7), this step is kinetically slowed down, in other words the process is shifted along the reactor axis increasing the moisture.

Conclusions

On the basis of the results obtained from the simulation of a slow pyrolysis biomass plant, it is possible to conclude that:

- temperature and residence time are two fundamental parameters that rule the pyrolysis process,
- results obtained at biomass flowrate of 1700 kg/h and residence time of biomass in the reactor of 30 minutes, clearly demonstrate that increase in temperature, helps in the advancement of chemical reactions; it is worth to note that up to 150 °C, the biomass does not undergo any degradation; above this temperature, the primary pyrolysis described by a first order reaction starts and continue till 300 °C; further increase in temperature results in the occurrence of secondary pyrolysis,
- isothermal pyrolysis at 1700 kg/h of biomass have shown that, at temperature of 350 °C, residence time of 30 minutes is enough to finish primary pyrolysis, but it does not appear to be sufficient to start secondary pyrolysis; whereas, at 500 °C, the secondary pyrolysis already starts at 3 minutes,
- results obtained from the model are in good agreement with the experimental data of the SICARB plant; the maximum relative errors of +5.1 and –3.5 were observed for water and carbon dioxide, respectively,
- products distribution and temperature profile along the axis of the reactor shows that the primary pyrolysis finishes at about 8 metres length (approx. 350 °C); from this point onward, the secondary pyrolysis clearly starts,
- the profile temperature has an inflection point at about 8 meters; it is mainly caused due to more endothermic primary pyrolysis compared to the secondary one, and
- lastly, it was also ascertained that the biomass moisture could delay the starting of the pyrolysis process.

Acknowledgments

The authors would like to express their sincere thanks to the reviewers and, especially, to Dr. Francesco Pistocchi for valuable suggestions during the preparation of this manuscript.

Nomenclature

A – frequency factor
C – concentration, [kmolm^{-3}]
c – specific heat, [Jkg^{-1}k^{-1}]
E – energy, [kJmol^{-1}]
K – equilibrium constant, [–]
k – kinetic constant, [–]
LHV – low heating value, [MJkg^{-1}]
P – partial pressure, [atm]
r – reaction rate, [kgmol^{-1} s^{-1}]
R – gas constant, [kJmol^{-1}K^{-1}]
T – temperature, [K]
H – enthalpy , [kJmol^{-1}]

Greek letters

Δ – variation
τ – time, [s]

Subscripts

a – activation
b – biomass
c – combustion
f – formation
p – constant pressure
daf – dry ash free

Superscripts

° – standard state

Acronyms

PFR – plug flow reactor
PM – molar mass, [kgkmol^{-1}]

References

[1] Bridgwater, A.V., Biomass Fast Pyrolysis, *Thermal Science, 8* (2004), 2, pp. 21-49

[2] Kung, H. C., A Mathematical Model of Wood Pyrolysis, *Combustion and Flame, 18* (1972), 2, pp. 185-195
[3] Miyanami, K., *et al.*, A Mathematical Model for Pyrolysis of a Solid Particle – Effects of the Heat of Reaction, *The Canadian Journal of Chemical Engineering, 55* (1977), 3, pp. 317-325
[4] Fan, L.T., *et al.*, A Mathematical Model for Pyrolysis of a Solid Particle – Effects of the Lewis Number, *The Canadian Journal of Chemical Engineering, 55* (1977), 1, pp. 47-53
[5] Peters, B., Bruch, C., Drying and Pyrolysis of Wood Particles: Experiments and Simulation. *Journal of Analytical and Applied Pyrolysis, 70* (2003), 2, pp. 233-250
[6] Alves, S., Figueiredo, J. L., A Model for Pyrolysis of Wet Wood, *Chemical Engineering Science, 44* (1989), 12, pp. 2861-2869
[7] Thurner, F., Mann, U., Kinetic Investigation of Wood Pyrolysis, *Industrial and Engineering Chemical Process Design and Development, 20* (1981), 3, pp. 482-488
[8] Shafizadeh, F., Chin, P. P. S., Thermal Deterioration of Wood, *ACS Symposium Series, 43* (1977), 5, pp. 57-81
[9] Shen, D. K., Modeling Pyrolysis of Wet Wood under External Heat Flux, *Fire Safety Journal¸ 42* (2007), 3, pp. 210-217
[10] Di Blasi, C., Heat, Momentum and Mass Transport through a Shrinking Biomass Particle Exposed to Thermal Radiation, *Chemical Engineering Science, 51* (1996), 7, pp. 1121-1132
[11] Broido, A., Evett, M., Hodges, G. C., Yield of 1,6-anhydro-3,4-dedeoxy-β-D-glyccrohex-3-enpyranos-2-ulose (levoglucosenone) on the Acid-Catalyzed Pyrolysis of Cellulose and 1,6-anhhydro-β-D-glucopyranose (levoglucosan), *Carbohydrate Research, 44* (1975), 2, pp. 267-274
[12] Bradbury, A.G.W., Sakai, Y., Shafizadeh, F., A Kinetic Model for Pyrolysis of Cellulose, *Journal of Applied Polymer Science, 23* (1979), 11, pp. 3271-3280
[13] Liden, A. G., Berruti, F., Scott, D. S., A Kinetic Model for the Production of Liquids from the Flash Pyrolysis of Biomass, *Chemical Engineering Communications, 65* (1988), 1, pp. 207-221
[14] Koufopanos, C. A., *et al.*, Modelling of the Pyrolysis of Biomass Particles. Studies on Kinetics, Thermal and Heat Transfer Effects, *The Canadian Journal of Chemical Engineering, 69* (1991), 4, pp. 907-915
[15] Srivastava, V. K., Sushil, Jalan, R. K., Prediction of Concentration in the Pyrolysis of Biomass Materials-II, *Energy Conversion and Management, 37* (1996), 4, pp. 473-483
[16] Jalan, R. K., Srivastava, V. K., Studies on Pyrolysis of a Single Biomass Cylindrical Pellet Kinetic and Heat Transfer Effects, *Energy Conversion and Management, 40* (1999), 5, pp. 467-494
[17] ***, Energy Research Centre of the Netherlands, Database for Biomass and Waste, http://www.ecn.nl/phyllis
[18] Della Rocca, P.A. *et al.*, Pyrolysis of Hardwood Residues: On Kinetics and Chars Characterization, *Biomass and Bioenergy, 16* (1999), 1, pp. 79-88
[19] Di Blasi, C., *et al.*, Product Distribution from Pyrolysis of Wood and Agricultural Residues, *Ind. Eng. Chem. Res., 38* (1999), 6, pp. 2216-2224
[20] Bonnefoy, F., Gilot, P., Prado, G., A Three-Dimensional Model for the Determination of Kinetic Data from the Pyrolysis of Beech Wood, *Journal of Analytical and Applied Pyrolysis, 25* (1993), June, pp. 387-394
[21] Wang, Y., Kinoshita, C. M., Kinetic Model of Biomass Gasification, *Solar Energy, 51* (1993), 1, pp. 19-25
[22] Di Blasi, C., Analysis of Convection and Secondary Reaction Effects within Porous Solid Fuels Undergoing Pyrolysis, *Combustion Science Technology, 90* (1993), 5-6, pp. 315-340
[23] Schmidt, L. D., The Engineering of Chemical Reactions, Oxford University Press, New York, USA, 1998
[24] Di Blasi, C., Dynamic Behaviour of Stratified Downdraft Gasifiers, *Chemical Engineering Science, 55* (1999), 15, pp. 2931-2944
[25] Sofialidis, D., Faltsi, O., Simulation of Biomass Gasification in Fluidized Beds Using Computational Fluid Dynamics Approach, *Thermal Science, 5* (2001), 2, pp. 95-105

Paper submitted: September 1, 2009
Paper revised: October 20, 2009
Paper accepted: September 16, 2010